Detection of rheumatoid arthritis using infrared imaging

Monique Frize[a,b], Cynthia Adéa[a], Pierre Payeur[b], Gina Di Primio[c], Jacob Karsh[d], Abiola Ogungbemile[a]

[a]Systems & Comp. Eng., Carleton University, 1125 Colonel By Drive, Ottawa, ON, Canada, K1S 5B6;
[b]School Inf. Tech. & Eng., University of Ottawa, Ottawa, ON, Canada, K1N 5N6;
[c]Medical Imaging, Ottawa Hospital, 501 Smyth, Ottawa, ON, Canada;
[d]Rheumatology, Ottawa Hospital, Riverside Dr., Ottawa, ON, Canada.

ABSTRACT

Rheumatoid arthritis (RA) is an inflammatory disease causing pain, swelling, stiffness, and loss of function in joints; it is difficult to diagnose in early stages. An early diagnosis and treatment can delay the onset of severe disability. Infrared (IR) imaging offers a potential approach to detect changes in degree of inflammation. In 18 normal subjects and 13 patients diagnosed with Rheumatoid Arthritis (RA), thermal images were collected from joints of hands, wrists, palms, and knees. Regions of interest (ROIs) were manually selected from all subjects and all parts imaged. For each subject, values were calculated from the temperature measurements: Mode/Max, Median/Max, Min/Max, Variance, Max-Min, $(\text{Mode-Mean})^2$, and Mean/Min. The data sets did not have a normal distribution, therefore non parametric tests (Kruskal-Wallis and Ranksum) were applied to assess if the data from the control group and the patient group were significantly different. Results indicate that: (i) thermal images can be detected on patients with the disease; (ii) the best joints to image are the metacarpophalangeal joints of the 2nd and 3rd fingers and the knees; the difference between the two groups was significant at the 0.05 level; (iii) the best calculations to differentiate between normal subjects and patients with RA are the Mode/Max, Variance, and Max-Min. We concluded that it is possible to reliably detect RA in patients using IR imaging. Future work will include a prospective study of normal subjects and patients that will compare IR results with Magnetic Resonance (MR) analysis.

Keywords: Infrared imaging, rheumatoid arthritis, joint temperatures, statistical significance tests.

1. INTRODUCTION

The prevalence of Rheumatoid Arthritis (RA) in Canada, as well as in the rest of the world, is about 0.5 to 1%. Within 10 years of diagnosis, 50% of patients have severe disability as well as a decreased life expectancy from 3 to 18 years. Early diagnosis of RA and initiation of aggressive therapy early in the course of the disease can diminish disease progression and, in some patients, even lead to drug free remission. Clinical signs of RA, pain and swelling of joints, are usually present and progressive. Swollen joints are among the criteria used to classify a patient as having RA and constitute the major indication for initiating therapy. Rheumatologists detect joint swelling by the classical examination technique. But in early stages of the disease, patients may suffer without apparent joint swelling and with negative radiographs. In these cases, techniques such as high resolution ultrasound (HRUS) or Magnetic Resonance (MR) imaging may reveal morphologic changes or hyperemia in the form of synovial thickening or enhancement and allow a much earlier diagnosis of RA. MR is quite expensive and in Canada has excessive wait times. HRUS is less expensive, but very time consuming and operator dependent.

The identification of biomarkers of disease severity and predictors of outcome are areas of active research. The intensity of the infrared signal may be useful as a measure of inflammatory load. Achievement of remission, or the decreased intensity of the infrared signal, may confirm adequacy of treatment. Infra-Red technology (IRT) may provide an

Medical Imaging 2011: Image Processing, edited by Benoit M. Dawant, David R. Haynor,
Proc. of SPIE Vol. 7962, 79620M · © 2011 SPIE · CCC code: 1605-7422/11/$18 · doi: 10.1117/12.874552

alternative to MR in defining radiographic remission, thus freeing up expensive imaging time for other patients. The long-term goal of this research project is to develop a low-cost, non-invasive technology, providing a quantitative assessment of RA, and allowing one to monitor therapy effectiveness.

2. LITERATURE REVIEW

Over the last two decades, traditional techniques such as bone scintingraphy, ultrasound, contrast enhanced US[1] and most recently MR, especially contrast enhanced MR, were used in two ways: first for early diagnosis, and second to assess the effectiveness of expensive and often fairly toxic therapies. However, MR remains incompletely accepted clinically[2,3,4].

Over the past fifty years, infrared imaging has been applied to many fields. The major limitations encountered in early work were its low resolution, the large size of sensors, and the limited power of computers for the image post processing[5]. Anecdotal clinical studies have demonstrated that heat distribution provides a quantitative measure of disease activity and especially of inflammation in knee joints[6,7,8]. In these studies, correlation has been observed between heat distribution measurement and physicians' clinical assessments. Early studies have mainly focused on knees and ankles to assess the effect of various treatments on RA patients. In our study, we analysed the temperatures of various joints in the hands, wrist, back of the hand, palm, thumb shaft, elbows, knees, feet and ankles, both for the control group and the patient group. To date, our analysis has been completed on the joints of the hand and the knee, the results of which are reported in this paper.

Anomaly detection in infrared images is a challenging task. Often the key element of an automated anomaly detection system is the segmentation of relevant information from noise and background. Numerous algorithms are available for the segmentation of visible images, but these differ significantly from infrared images. The intensity of the latter depends on object temperature and surface properties, surface orientation, wavelength, and is not necessarily uniform across an object, even if the temperature of that object is uniform. The environmental conditions at the time of imaging also influence the resulting images. Moreover, the range of intensity of infrared images is typically much less than for visible images, leading to low contrast, poor resolution, and less texture information. Key features that are successfully used in the processing of visible images cannot be used reliably when dealing with infrared images, thus the segmentation of the latter presents unique challenges and depends greatly on the application considered. For example, methods developed for automated tracking of military targets[9] or for manufacturing quality control[10] do not perform well when translated to applications in medicine.

Our group introduced a method based on morphological processing of edge maps using both strong and weak edges to recover the contour of faint parts of the object in low contrast and high noise situations[11,12,13]. Promising results were obtained for synthetic images of hands on three types of real backgrounds. The segmentation approach is part of a larger framework for automated identification of abnormal human regions in infrared images and will be integrated into this project at a later stage. To date, we have applied IRT measurements to the assessment of pain[14], of musculoskeletal disorders in the arms and hands of computer users, and to capture the evolution of the temperature distribution on pianists' hands and arms during practice[15].

Human movement monitoring systems are widely used to study gait analysis during training and rehabilitation of patients and to provide diagnostic tools. But current motion capture techniques used by professionals are costly, tedious to set up, and rely on markers mounted on subjects. Recent advances in markerless body tracking[16] solutions offer greater flexibility for application in a clinical setting, allowing operation in usual indoor environments with no intervention on the subject by the operator. Our team has been successful at developing such markerless motion capture systems to monitor the entire body motion[17]. Such solutions can be adapted and refined to address, with higher accuracy, the specific characteristics of joints in the hand, arm or leg in order to obtain precise measurements on the extent of motion.

Gomez *et al*.[18] developed an integrated imaging system to obtain accurate and reproducible multi-spectral dermatological images. This system can collect up to 10 different spectral bands (Ultraviolet to Infrared) and was developed to allow comparative studies of a time series of images, showing that a multi-spectral approach can be used successfully to segment lesions and track the evolution of dermatological diseases. But, this system does not incorporate motion capture.

In this first phase of the research project, we report on the completion of three objectives: The first was to determine if it was possible to discriminate between the average temperature of joints of a control group and of a group of patients diagnosed with RA; the second was to identify which of the joints measured and analyzed best confirm the presence of RA; the third was to identify which of the calculated values such as: Mode/Max, Mode/Min show a significant statistical difference between the temperature of joints of patients and of the control group (normal subjects).

Ultimately, the final prototype is expected to allow tracking of the evolution of RA diseases using only IRT and visual imaging. The approach is based on the fact that painful areas tend to have different temperature distributions than healthy ones. It also precisely quantifies the extent to which a patient can move his/her fingers and limbs, providing comparative data over time as the disease is being treated. In this holistic fashion, the user-friendly system will produce meaningful imagery that can be easily interpreted by radiologists and rheumatologists.

3. METHODOLOGY

3.1 Data collection

Thirteen patients (nine females and four males) diagnosed with rheumatoid arthritis, and eighteen control subjects (8 females and ten males) between the age of 19 and 70 were recruited after receiving Research Ethics Board approval from The Ottawa Hospital and from the two universities concerned (Carleton and Ottawa). All subjects followed a study protocol which requested that they not use talcum powder, lotion, or deodorant on the skin on the day of the session; not to consume alcoholic beverages twelve hours prior, and not to consume hot beverages at least one hour prior to the session; not to be subject to acupuncture, transcutaneous electrical nerve stimulation, hot or cold presses, or any form of physiotherapy for at least twenty-four hours prior to the session. They were not to do intense physical exercises at least four hours prior to the tests, avoid prolonged sun exposure for a week, not smoke for at least two hours prior to the testing, and not wear any rings, necklaces, or bracelets during the session. The room had a controlled temperature of around 20 degrees C, there were no windows, and all subjects wore short-sleeved T-shirt and shorts, removed their shoes and socks when they arrived in our laboratory, and were seated with no parts of their body touching other parts for fifteen minutes. This was to cool the parts of the body that were covered by clothing and have everyone in the same condition prior to the imaging session.

The IR camera uses a solid state uncooled microbolometer focal plane array of 320×420 pixels, operating in the 7.5μm−13μm range, with a 24mm germanium lens with an anti-reflective coating providing a 24°x18° field of view with a minimum focus distance of 30 cm. Its spatial resolution is 1.3mrad and thermal resolution is 0.05°C at 30°C. The camera was connected to a laptop via a Firewire interface, thereby capturing sequences of 14bit digital thermal images at a set speed of 30 frames per seconds. Images were taken of the hands (dorsal and palm), elbows, knees, ankles, and feet. To date, the analysis focused on the joints of the hands and the knees. Figure 1 shows the joints of the hand with the name of each joint: Metacarpal phalangeal (MCP) joints; Metacarpal phalangeal joint of the third finger (MCP3); the third Proximal interphalangeal joint (PIP3); the third Distal interphalangeal joint (DIP3); and the Middle Phalanx (MP).

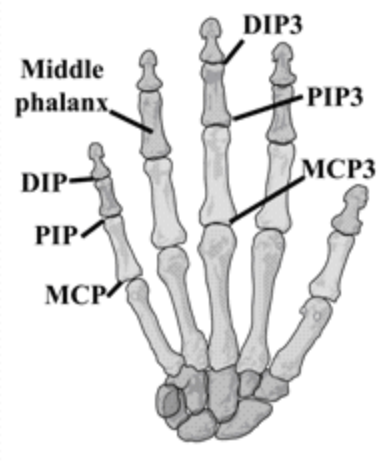

Figure 1: Joints of a hand with names of joints

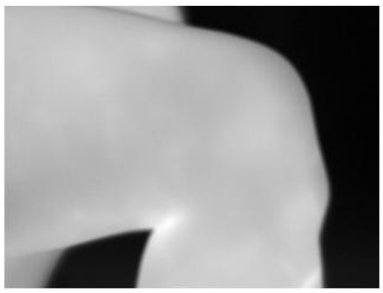

Figure 2: Anterior view of the flexed knee in the median plane

Images of the extended knees were taken in the posterior and anterior view of the frontal anatomical plane. Images were taken of both extended knees at one time and of individual extended knees separately (see Figure 2 for an example of the image of a single knee). Images were also captured in the sitting position (knees flexed at 90 degrees) in the anterior frontal view. Captions were taken of both flexed knees at one time and of individual flexed knees separately. The individual flexed knees were also imaged in the right and left median plane.

3.2 Data analysis

The analysis of the hand was focused on the 2nd and 3rd MCPs (Metacarpal Phalangeal joints of the index and middle fingers), the 2nd and 3rd PIPs (PIP joints of the index and middle fingers), the wrist, the back of the hand, and the palm. For the palms, the standard diameter was 120 pixels, which corresponded to approximately 4 cm in diameter. The Regions of Interests (ROIs) were manually selected from the gray scale images, using anatomical reference points, to determine the location of the synovial membrane. The gray scale images provide temperature values between 0 and 1. Figure 3 shows the manual selection of the regions of interest (ROIs) for the hand which are located respectively over the 2nd and 3rd MCPs and PIPs as well as over the wrist area.

Once the joints were identified, MATLAB[19] produced an array of temperature values which represented the temperature of every pixel within the selected region of interest of the IR image. The resulting array is a probability distribution of a real-valued random variable. Measurements were then extracted from these arrays to be analysed: max, min, mean, median, mode, standard deviation, skewness and kurtosis. The max and min measurements refer to the maximum and minimum temperatures within the array of the joint. The mean is the average temperature value of the elements of the array. If there are N elements in the array then the mean value is the sum of all element temperatures divided by N. The median is the temperature value of the middle element of the joint's array when all the elements of the array are arranged in either ascending or descending order according to their temperature values. If there are N elements in the array, the median is the value of the (N+1)/2 element of the ordered values of the array. The mode is the temperature value that occurs most frequently in the array of the joint. The mean, median and mode are measures of central tendency – the location of a distribution. The standard deviation is a measure of dispersion and refers to the variability of the array distribution around the mean value. The skewness and the kurtosis describe the shape of the distribution. The skewness is a measure of the asymmetry of an array's distribution. A symmetric distribution around its mean has zero skewness and equal values of mean, median and mode. A distribution is positively skewed if the right tail is longer with mean > median > mode. A distribution is negatively skewed if the left tail is longer with mode > median > mean[20]. The kurtosis is a description of the peak of the array's distribution. A mesokurtic distribution has zero excess kurtosis and has a normal peak around the mean. An example of a mesokurtic distribution is the normal Gaussian distribution. A

distribution that is leptokurtic has a positive excess kurtosis and has a more acute peak around the mean with fatter tails. An example of a leptokurtic distribution is the Laplace distribution. A platykurtic distribution has a negative excess kurtosis and has a lower wider peak around the mean with thinner tails. An example of a leptokurtic distribution is the Bernoulli distribution[20].

Certain measurements extracted from the IR images, such as: max, min, mean, median, mode, are subject to inter-participant variation and many other factors such as time of day, vascular circulation of the patient, and the environment. Ratios, differences, and dispersion measurements (variance) were used to compare the control samples and the patient samples. Ratios, differences, and dispersion measurements are based on the thermal distribution of the surface of the skin rather than the exact temperature reading, thus eliminating inter-participant differences. The calculations used for the final analysis were: Skewness, Kurtosis, Variance, Mode/Max, Median/Max, Min/Max, Max-Min, $(\text{Mode-Mean})^2$, Mode/Min, Median/Min, Mean/Min.

The calculations for the control group included thirty-six measurements for each joint type (18 control subjects with a right and a left side imaged per joint); for the patient group, the calculations included twenty-six measurements (13 patient images of the right and the left sides). It is important to mention that RA is an auto-immune disease which usually affects joints bilaterally. Eight of the calculated series listed above were randomly selected and tested to see if they followed a normal distribution or not. The Lilliefors Test of normality[19] was applied to the each of the eight calculated series to see if their distribution was Gaussian. If the calculated series were normally distributed, parametric tests such as the Student t-Test and the Anova Test could be used to assess the statistical significance of the results. However, since all of these series did not follow a normal (Gaussian) distribution, non-parametric tests, such as the Kruskal-Wallis Test[19,20], and the Ranksum Test[19], were used to establish whether the temperature measurements of the control group and those of the patient group were statistically different. Since all eight series of calculated values were found not to have a normal distribution, we assumed that all the remaining series followed this pattern and concluded that parametric tests would not be used for any of the statistical analyses. Table 1 shows four outputs obtained by the normality test. The null hypothesis of the test is that the distribution of the calculated values belongs to the normal distribution family; therefore, if h is 1 with a p-value lower than α (where $\alpha = 0.05$), it is possible to conclude that the distribution of the calculated values is not a normal distribution.

Participant Type	Joint	Matrix Distribution	MATLAB Outputs			
			h value	p value	KS value	Critical Value
Control Subjects	2nd MCP	Skewness	1	0.0482	0.1503	0.1497
	3rd MCP	Kurtosis	1	0.0020	0.1955	0.1497
	2nd PIP	Variance	1	0.0026	0.1920	0.1497
	3rd PIP	Minimum Temperature	1	0.0040	0.1865	0.1497
Patients	2nd MCP	Kurtosis	1	0.001	0.4422	0.1699
	3rd MCP	Kurtosis	1	0.0346	0.1767	0.1699
	2nd PIP	Maximum Temperature	1	0.0019	0.2226	0.1699
	3rd PIP	Minimum Temperature	1	0.0133	0.1932	0.1699

Table 1: MATLAB Lilliefors Test Results for Randomly Selected Matrices

4. RESULTS AND DISCUSSION

4.1. Results for the first objective

This investigation aimed at defining whether it is possible to discriminate between the average temperature of joints of a control group and a group of RA patients: Table 2 shows MATLAB's Ranksum test results, comparing the control group

and the patient group temperatures for the hand joints and the knee. Where the h value is 1, for the various tests listed, the temperature difference between the two groups for that particular joint or knee is significant. From these results, we can conclude that it is possible to discriminate between the control group and the patient group. The Skewness, Mode/Max, and Mode/Min values of the 2nd MCP had statistically different distributions for the control group and for the patient group. Moreover, the Standard Deviation (STD), Mode/Max, Median/Max, Min/Max, Variance, Max-Min, $(\text{Mode-Mean})^2$, and Mean/Min values of the 3rd MCP showed a statistical difference between the distribution of the data in the control and patient groups. The control group's Kurtosis value for the 3rd PIP was also statistically different than the patient's Kurtosis value for this joint. The STD, Min/Max, Variance, Max-Min, Mode/Min, Median/Min, and Mean/Min values for the knee were also statistically different for the control and patient groups.

The grayscale images of the normal group for the knee showed a gradient that was uniform and positive from the patella to the inside of the flexed knee. In other words, the patella region has a low temperature, and this temperature increases as you get closer to the inside of the flexed knee, where the temperature is the warmest. Moreover, there were no hot regions within the ROIs of the control group subjects. Examining the results for the patient group, the temperature distribution gradient from the patella to the inside of the flexed knee was not always uniform or positive. In many cases, the temperature gradient showed some spikes and was negative; there were also hot spots throughout the joint. Thus grayscale images of patients with RA show a non-uniform temperature gradient and the presence of hot regions. The non-uniform and negative thermal gradients seen in the RA patients' images can be explained by increased vascularity caused by synovitis and the proliferation of the synovial cells (the pannus). Blood is also shunted from the deep circulation to the subcutaneous circulation, adding to the increase in temperature at the surface of the joint. In RA, there are also chemical mediators and an increase in chemical activity within the intra-articular joint due to the inflammation process. These pathophysiological aspects can explain the abnormalities seen in the patients' infrared images.

Joint	Calculated values	p-value	h value
MCP2	STD	0,3828	0
	Skewness	0,0136	1
	Kurtosis	0,9346	0
	Mode/Max	0,0105	1
	Median/Max	0,0654	0
	Min/Max	0,7484	0
	Variance	0,3828	0
	Max-Min	0,8171	0
	$(\text{Mode-Mean})^2$	0,8521	0
	Mode/Min	0,0173	1
	Median/Min	0,2861	0
	Mean/Min	0,4603	0
MCP3	STD	0,0153	1
	Skewness	0,4786	0
	Kurtosis	0,1969	0
	Mode/Max	0,0212	1
	Median/Max	0,0361	1
	Min/Max	0,0047	1
	Variance	0,0153	1
	Max-Min	0,0074	1
	$(\text{Mode-Mean})^2$	0,011	1
	Mode/Min	0,4786	0

Joint	Calculated values	p-value	h value
PIP2	STD	0,9346	0
	Skewness	0,1417	0
	Kurtosis	0,0962	0
	Mode/Max	0,2476	0
	Median/Max	0,2356	0
	Min/Max	0,6599	0
	Variance	0,9346	0
	Max-Min	0,5912	0
	$(\text{Mode-Mean})^2$	0,2298	0
	Mode/Min	0,2021	0
	Median/Min	0,2356	0
	Mean/Min	0,2241	0
PIP3	STD	0,7484	0
	Skewness	0,3360	0
	Kurtosis	0,0011	1
	Mode/Max	0,3993	0
	Median/Max	0,3285	0
	Min/Max	0,4694	0
	Variance	0,7484	0
	Max-Min	0,4162	0
	$(\text{Mode-Mean})^2$	0,0612	0
	Mode/Min	0,4603	0

	Median/Min	0,1055	0		Median/Min	0,7371	0
	Mean/Min	0,0289	1		Mean/Min	0,7371	0
				Knee	STD	0,0341	1
					Skewness	0,1585	0
					Kurtosis	0,2508	0
					Mode/Max	0,2226	0
					Median/Max	0,0318	0
					Min/Max	0,0027	1
					Variance	0,0341	1
					Max-Min	0,0026	1
					$(\text{Mode-Mean})^2$	0,6635	0
					Mode/Min	0,0072	1
					Median/Min	0,0069	1
					Mean/Min	0,0128	1

Table 2: MATLAB's Ranksum test results, comparing the h value for several statistical tests done for each of the joints measured; an h value of 1 indicates a significant difference between the two groups (control subjects and patients).

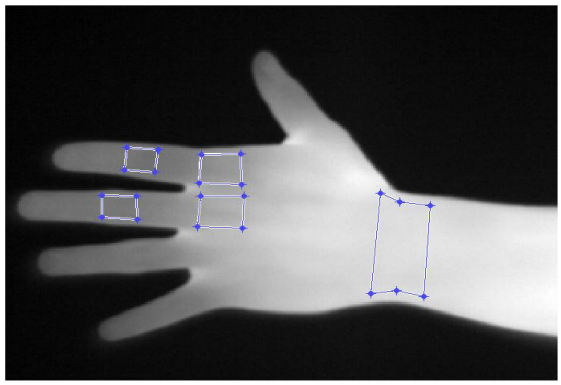

Figure 3: Regions of interest selected in the hand

4.2. Results for the second objective

The goal of the second task was to identify the joints that best determine if a subject is normal or has RA. From the Ranksum hypothesis test results in Table 2, we concluded that the Mode/Max data calculated for the 2nd PIP, the 3rd PIP, and the wrist could not differentiate between the control group and the patient group. Only the Kurtosis for the 3rd PIP showed statistically significant results. The joints that best distinguish between the control and the patient groups were the 2nd MCP, the 3rd MCP, and the knee, with a significance level of 0.95. These results do not include the assessment of the elbows, the ankles, and the feet.

Histograms in Figure 4 (2nd MCP) and Figure 5 (3rd MCP) show that the bins containing the most elements for the control group are never the same as the bins containing the most elements for the patient group. For example, we see in Figure 4 that the Mode/Max for the 3rd MCP for the control group is shifted to the left, whereas the patients' Mode/Max is shifted to the right. The bin containing the most elements in the control group's data is the bin value 0.9895, whereas the bin containing the most elements in the patient group's data had a value greater than 0.9975. Thus the Mode/Max distribution for the 3rd MCP can distinguish well between the control and patient groups.

The histogram in Figure 6 shows that the variance for the knee of the control subjects is shifted to the right whereas the patients' variance is shifted to the left. The bin containing the most elements in the calculated values of the control group is the 0.385 bin whereas the bin containing the most elements in the calculated values of the patients is the 0.205 bin. It is clear from the histogram above that the distributions of the variance analysis can distinguish between the control and patient groups.

The wrist was taken from the posterior view of the frontal plane. The results confirmed a previous report[21] that the wrist showed the smallest temperature difference between the control and the patient groups. Our work confirms that the MCPs and the knees are the best joints to assess in a clinical setting to determine if a participant has RA. Of course, future analysis of the other joints measured, such as elbows, ankles, and feet may modify this conclusion in the future.

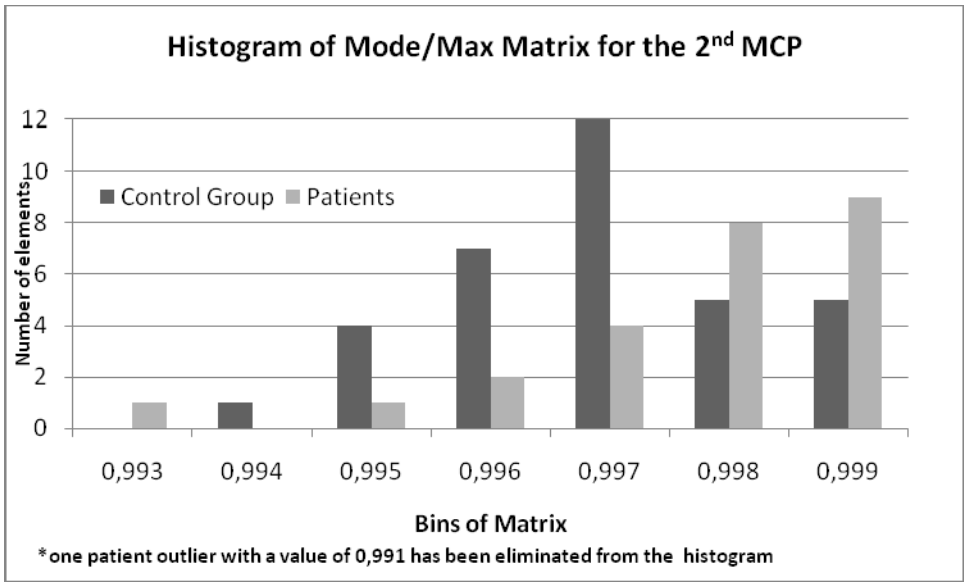

Figure 4: Histogram of Mode/Max calculated values for the 2nd MCP for patient and control groups.

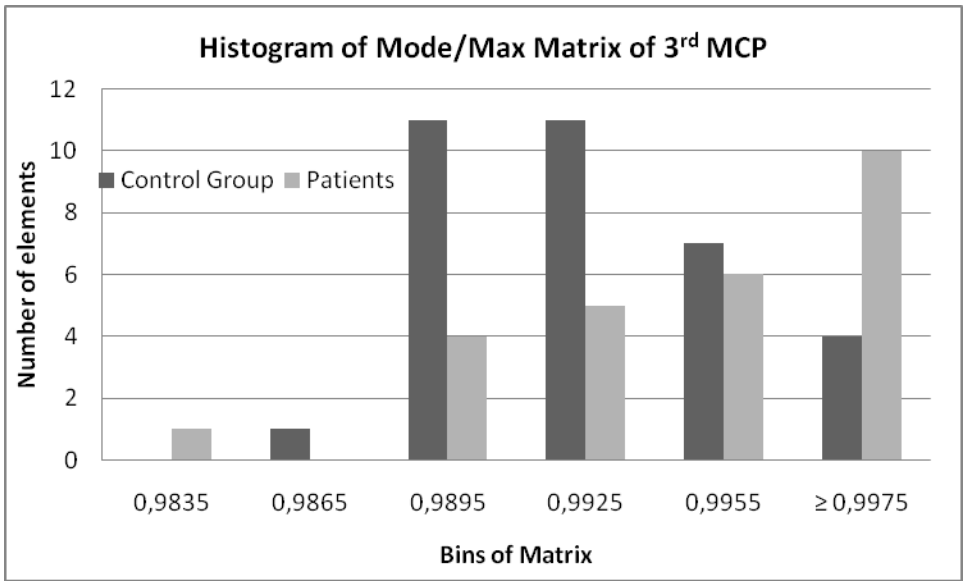

Figure 5: Histogram of Mode/Max for the 3rd MCP of the control group and of the patient group

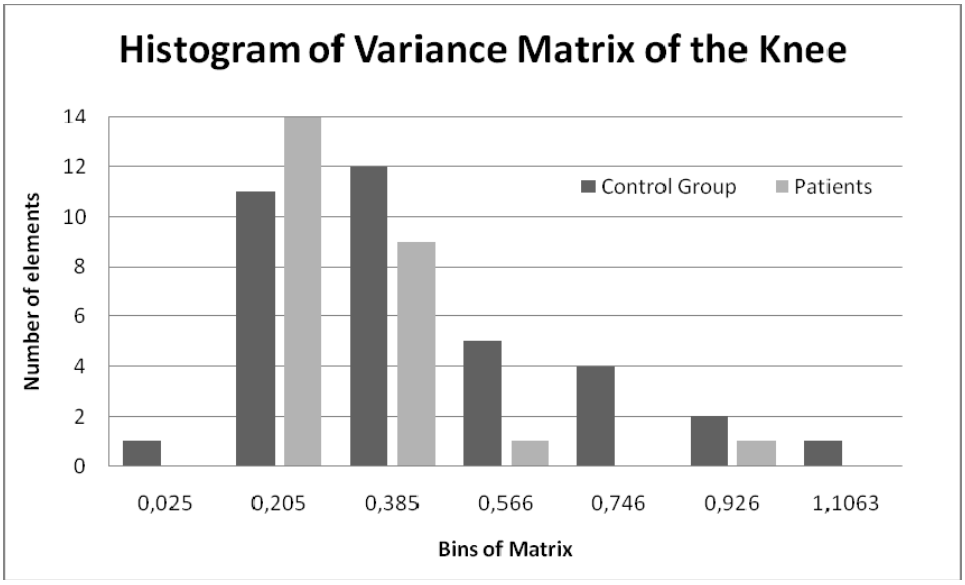

Figure 6: Histogram of the calculations of Variance for the Knee of the control and patients groups

4.3. Results for the third objective

The last component of this investigation was to identify which of the calculated values best discriminate between the temperatures measured with the control group and those measured with the patient group:

The calculations which resulted in a statistical difference between both groups were Max-Min, the Variance (STD Squared), and the ratio Mode/Max. The Max-Min and the Variance represent the range and the dispersion of the thermal distribution within the joint. The Mode/Max represents abnormally hot regions that characterize the presence of RA.

The infrared images for RA patients are characterised by their non-uniform thermal distribution and by the presence of hot spots. The presence of a hot spot increases the value of the mode temperature, thus making the patients' Mode/Max generally smaller than that of the control group. Thus we can conclude that the Mode/Max, the Variance and the Max-Min calculations for the MCPs and the knees were able to discriminate well between the control group and the patient group, and appear to be the best approaches to discriminate between the two groups.

5. CONCLUSION AND FUTURE WORK

This study enabled us to establish a proof of concept that infrared thermal imaging can detect the presence of RA in human subjects. Moreover, the work enabled us to conclude that, of the joints analysed in this first phase of the project, the metacarpal phalangeal joint of the index and middle fingers and the knee best indicate the presence or absence of RA, when compared to the wrist, palm, thumb, proximal interphalangeal joints, and distal interphalangeal joints. The calculated values that best discriminate between the temperature measurements of the control and patient groups were: the Mode/Max, the Variance, and the Max-Min calculations.

Future work includes completing the analysis of the other joints that were imaged with the two groups (elbows, ankles, and feet). It will also attempt to automate the segmentation and the analysis of joints. We also plan to classify patients in three categories of RA activity (low, medium, and high) through the application of pattern classification approaches such as decision trees and artificial neural networks. A complementary approach of visual data is also being developed to simultaneously collect motion data on the limbs being examined using markerless motion capture technologies. The study of the correlation between the findings presented in this work and that related to the maximal extent of joint movement respectively in normal subjects and patients will contribute to refine the analysis and make the proposed diagnostic tool more robust. The prototype that results from these efforts will be prospectively tested in a real clinical environment and use will be made of MR examinations and their interpretation as gold standard[22] to compare the results and classification of our new prototype.

6. ACKNOWLEDGMENT

The authors wish to sincerely thank the 18 volunteers and 13 patients who participated in this study, as well as acknowledge the contribution of the Natural Sciences and Engineering Research Council of Canada to the development of the necessary research infrastructure.

7. REFERENCES

[1] P.P. Cheung, M. Dougados, L. Gossec. "Reliability of ultrasonography to detect synovitis in rheumatoid arthritis: a systematic literature review of 35 studies (1,415 patients)" Arthritic Care Res (Hoboken). 2010 Mar; 62(3):323-34. Review. PMID: 20391478 [PubMed-indexed for Medline]

[2] J.E. Freeston, P. Bird, P.G. Conaghan. "The role of MRI in rheumatoid arthritis research and clinical issues." Curr Opin Rheumatol. 2009 Mar; 21(2):95-101. Review. PMID:19339918 [PubMed-indexed for Medline].

[3] F. McQueen, M. Ostergaard, C. Peterfy, M. Lassere, B. Ejbjerg, P. Bird, P. O'Connor, H. Genant, R. Shnier, P. Emery, J. Edmonds, P. Conaghan, "Pitfalls in scoring MR images of rheumatoid arthritis wrist and metacarpophalangeal joints". *Ann Rheum Dis*. 2005 February; 64(Suppl 1): i48–i55. doi: 10.1136/ard.2004.031831.

[4] M.A. Cimmino, M. Parodi, E. Silvestri et al. "Correlation between radiographic, echographic and MRI changes and rheumatoid arthritis progression." Reumatismo, 2004 Jan-Mar; 56(1 Suppl 1): 28-40. Italian. PMID: 15201938 [PubMed-indexed for Medline]

[5] M. Aubry-Frize, G.R.C. Quartey, H. Evans, D. LaPalme, "The Thermographic Detection of Pain". *Proc. 3rd Canadian Clinical Engineering Conf.*, pp. 82-83, Saskatoon, SK, 1981.

[6] Collins, A.J., Ring, E.F.J., Cosh, J.A. and Bacon, P.A. "Quantification of Thermography in Arthritis Using Multi Isothermal Analysis", Annals of the Rheumatic Diseases, Vol. 33, pp. 113-115, 1974.

[7] M.D. Devereaux, G.R. Parr, D.P. Page Thomas, B.L. Hazleman, "Disease Activity Indexes in Rheumatoid Arthritis; a Prospective, Comparative Study with Thermography", *Annals of Rheumatic Diseases*, Vol. 44, pp. 434-437, 1985.

[8] De Silva, M., Kyle, V., Hazelman, B., Salisbury, R.S., Page-Thomas, D.P., and Wraight, P. "Assessment of Inflammation in the Rheumatoid Knee Joint", Annals Rheumatic Diseases, Vol. 45, pp. 277-280, 1986.

[9] Ernisse, B., Rogers, S.K., DeSimio, M.P., and Raines, R.A. "Complete automatic target cuer/recognition system for tactical forward-looking infrared images," Optical Engineering, vol. 36, pp. 2593–2603, September 1997.

[10] Huang, S.Y., Mao, C.W., and Cheng, K. "A vq-based approach to thermal image analysis for printed circuit boards diagnosis," IEEE Trans. Instrum. Meas., vol. 54, pp. 3281–2388, Dec. 2005.

[11] Herry, C.L., Goubran, R.A., and Frize, M. "Segmentation of infrared images using cued morphological processing of edge maps," in Proc. IEEE Instr. Meas. Tech. Conf., Warsaw, May 2007.

[12] Herry, C.L., Frize, M., and Goubran, R.A. "Search for abnormal thermal patterns in clinical thermal infrared imaging," in Proceedings of the IEEE International Workshop on Medical Measurements and Applications MeMeA, Ottawa, Ontario, Canada, May 2008.

[13] Herry, C.L., Goubran, R.A., and Frize, M. (2008) "Improving the Detection and Localization of Anatomical Landmark Points in Infrared Images Using Symmetry and Region Specific Constraints". Proceedings of the 25th IEEE International Instrumentation and Measurement Technology Conference (I2MTC08), Victoria, BC, May 2008.

[14] Herry, C.L., and Frize, M. "Quantitative assessment of pain-related thermal dysfunction through clinical digital infra-red thermal imaging." Biomedical Engineering Online 2004, 3:19.

[15] Herry C.L., Frize M., Goubran R.A., Comeau G. (2007) "Etude thermographique de pianistes lors d'une séance de travail: évolution de la température superficielle des muscles et premières interprétations", Recherche en Education Musicale, No. 24, August 2006: 89-104.

[16] Caillette, F. "Real-Time Markerless 3-D Human Body Tracking", PhD thesis, U. Manchester, 2006.

[17] Bériault, S., Côté, M., and Payeur, P. "Volumetric Modeling with Multiple Cameras for Markerless Motion Capture in Complex Scenes". Proceedings of the IEEE International Instrumentation and Measurement Technology Conf. I2MTC08), pp. 359-364, Victoria, BC, May 2008.

[18] Gomez, D.D., Carstensen, J.M., Ersbell, B.J. **"**Precise Multi-Spectral Dermatological Imaging", *Nuclear Science Symposium Conf. Rec.,* Vol.5, Iss. 16-22, pp. 3262- 3266, 2004.

[19] Salvatore, D. and D. Reagle. "Theory and Problems of Statistics and Econometrics – Second Edition." Schaum's Outline Series of McGraw-Hill Companies, 2002.

[20] Matlab R2009a. Software – help files. Version 7.8.0.347, Mathworks 2009.

[21] Frize, M., Karsh, J., Herry, C.L., Adéa, C., Aleem, I., Payeur, P. (2009) Preliminary Results of Severity of Illness Measures of Rheumatoid Arthritis Using Infrared Imaging. Proc. MeMeA (Medical Measurements and Applications). Cetraro, Italy, May: 187-192.

[22] Conaghan, P.G., Bird, P., McQueen, F. et al. "The OMERACT MRI inflammatory arthritis group: advances and future research priorities." J. Reumatol. 2009 Aug; 36(8):1803-5, PMID: 19671816 [PubMed-indexed for Medline].